



Properties of yttrium-doped barium zirconate ceramics synthesized by the oxidant-peroxo method

M.D. Gonçalves, R. Muccillo*

Center of Science and Technology of Materials, Energy and Nuclear Research Institute, Travessa R 400, Cidade Universitária, S. Paulo, SP 05508-900, Brazil

Received 1 June 2013; received in revised form 23 June 2013; accepted 23 June 2013
Available online 29 June 2013

Abstract

Polycrystalline powders of yttrium-doped barium zirconate with nominal composition $\text{BaZr}_{0.9}\text{Y}_{0.1}\text{O}_{3-\delta}$ (BZY10) were synthesized by the oxidant-peroxo (OP) method using hexahydrated yttrium nitrate, barium nitrate and hydrated zirconyl nitrate. This is an environmental friendly method, free of common contaminants such as carbon graphite or halides, and promotes the formation of stoichiometric powders composed by sinteractive nanoparticles. The powders were amorphous and required a heat treatment to crystallize the perovskite phase. The powders were characterized by thermogravimetry and differential thermal analysis, X-ray fluorescence spectroscopy, X-ray diffraction, evaluation of specific surface area by inert gas adsorption, scanning electron microscopy and electrochemical impedance spectroscopy. Stoichiometric single perovskite BZY10 powders were successfully synthesized. Carbonate ions, adsorbed during the powder synthesis, are fully decomposed after calcination at 1200 °C. The powders consist of agglomerate reactive nanosized particles. Pressing the powders to pellets and sintering at 1600 °C yielded relative density higher than 91% of the theoretical density. Scanning electron microscopy images of chemically and thermally etched surfaces clearly defines two regions: one dense with grains of irregular shapes and average submicron size, and another porous. The impedance spectroscopy analysis shows that sintered pellets prepared with OP powders have higher electrical conductivity than pellets using powders obtained by solid state reaction.

© 2013 Elsevier Ltd and Techna Group S.r.l. All rights reserved.

Keywords: Oxidant-peroxo method; Powder synthesis; Proton conductor; Barium zirconate

1. Introduction

Solid oxide fuel cells (SOFCs) have attracted increasing interest due to their high conversion efficiency of chemical energy into electricity with low environmental impact, comparing to combustion-based technologies [1,2]. The most developed and already commercially available SOFC is based on oxygen-ion conducting solid electrolyte and the operational temperature is in the 800–1000 °C range [3–5]. Many efforts have been done to reduce the SOFC working temperature to an intermediate range (500–700 °C) to improve the cell lifetime and the components thermal expansion compatibility [1,6,7]. Proton conducting oxides have been proposed as candidates for these devices [2] due to their higher electrical conductivity

at intermediate temperatures [2,8]. Furthermore, SOFC devices with proton conductor solid electrolytes allow for fuel utilization with improved efficiency since water is generated at the cathode site [9,10]. Proton conductors based on yttrium-doped barium zirconate show relatively high proton conductivity at intermediate temperatures and chemical stability in carbon dioxide rich atmosphere [11,12]. Yttrium-doped barium zirconate powders synthesized by the conventional ceramic method (solid state reaction of cation oxides or carbonates) require high sintering temperatures or sintering aids to obtain dense pellets for use in electrochemical devices like humidity sensors and solid oxide fuel cells [13,14]. Wet-chemical routes, on the other hand, have been used to produce powder particles with higher sinterability to obtain low temperature sintered dense pellets [13,15–20].

The oxidant-peroxo (OP) method is here proposed for the synthesis of yttrium-doped barium zirconate powders for the

*Corresponding author. Tel.: +55 11 31339203.

E-mail addresses: muccillo@usp.br, rmuccillo@gmail.com (R. Muccillo).

following reasons: it is free of potential contaminants such as carbon and halides [21,22] and the powders consist usually of stoichiometric sinterable nanosized particles [23–25]. The idea is to produce yttrium-doped barium zirconate powders easily sinterable to avoid (i) high sintering temperatures and long times to produce dense ceramic bodies [13,14,26] and (ii) the barium losses that causes reduction of the electrical conductivity [13]. Several propositions have been set forth to improve chemical stability, sintering conditions and electrical conductivity of yttrium-doped barium zirconate, for example rare earth co-doping [27–29].

This paper describes the detailed procedure for the synthesis of yttrium-doped barium zirconate powders by the oxidant-peroxo method. The microstructural and the electrical characterization of the sintered pellets are also described.

2. Experimental

The single phase 10 mol% Y-doped barium zirconate (BZY10 hereafter) was synthesized by the oxidant-peroxo (OP) method and by the conventional solid state reaction (SSR) route. For the SSR route the starting materials were barium carbonate (99% BaCO₃, Vetec), yttrium oxide (99.9% Y₂O₃, Alfa Aesar) and zirconium oxide (99.9% ZrO₂, Alfa Aesar). The dried oxides, weighed according to the stoichiometry molar ratio, were thoroughly mixed with isopropyl alcohol (C₃H₈O) in an agate mortar, dried and calcined twice at 1250 °C for 24 h with an intermediate de-agglomeration step in an agate mortar. X-ray diffraction measurements were carried out after each step, to ascertain the formation of the cubic perovskite phase, in a Bruker-AXS D8 Advance diffractometer with Cu-K α radiation, in the 2θ range from 10° to 90° with 0.05° step size and 2 s per step.

The starting materials for the synthesis by the OP method were barium nitrate (99.9% BaNO₃, Aldrich), hexahydrated yttrium nitrate (99.9%, Y(NO₃)₃ · 6H₂O Aldrich) and hydrated zirconyl (IV) nitrate (99.99%, ZrO(NO₃)₂ · xH₂O Aldrich), with previous gravimetric analysis by heating at 900 °C for 2 h to estimate the molar quantity of Zr (IV) ions per gram of the reagent. All chemical reagents were used as received. All cation nitrates were weighed according to the stoichiometry molar ratio and then dissolved separately in distilled water. The final concentrations (mol/L) of the solutions are 3.62×10^{-2} , 3.26×10^{-2} and 3.6×10^{-3} for Ba²⁺, Zr⁴⁺ and Y³⁺, respectively.

50 mL of hydrogen peroxide (H₂O₂, analytical grade, Synth) were added to the zirconium solution to obtain the soluble zirconium peroxo-complex (ZrO(O₂)H⁺). All cation solutions were mixed together and rapidly added into an oxidant mixture (pH=11) of 130 mL of hydrogen peroxide and 50 mL of aqueous ammonia solution (analytical grade) under stirring and cooling in an ice-water bath. A white precipitate was immediately formed and was kept at rest for 24 h. Afterwards the precipitate was filtered and washed with a diluted ammonia solution to eliminate nitrate ions, dried at 90 °C for 12 h and ground in an agate mortar. This powder will be referred to as “precursor powder”.

Thermogravimetric and differential thermal analyses of the precursor powder were performed in a Netzsch STA 409E simultaneous thermal analyzer. The precursor powder (2.50 g) was calcined at 700, 800 and 900 °C for 4 h and at 1200 °C for 2 h with 10 °C min⁻¹ heating rate in zirconia crucibles with lids.

About 0.25 g of the BZY10 powders obtained by both OP method and SSR route were pressed uniaxially at 18 MPa and isostatically at 200 MPa to obtain 5 mm diameter, 5 mm thickness pellets. The green density was approximately 40% TD (Theoretical Density=6.2 g cm⁻³). To avoid barium volatilization the pellets were embedded in 10 mol% Ba excess BZY10 powder and sintered at 1600 °C for 4 h with 3 °C min⁻¹ heating and cooling rates. The relative densities of the sintered pellets were evaluated by the Archimedes method with kerosene as liquid medium.

X-ray diffraction measurements (Bruker-AXS) were carried out to determine the structural phase of all precursor powders as well as of heat treated powders and sintered pellets produced by both OP and SSR routes. Lattice parameters were evaluated with the Unit Cell software [30]. The stoichiometric ratio of the cations was evaluated by X-ray fluorescence analyses (Shimadzu EDX-720).

All powders were observed in a scanning electron microscope (Philips, XL30). Observations on polished (diamond paste down to 1 μ m) and chemically etched (boiling H₂SO₄ for 2 min) surfaces of sintered pellets were also carried out in a scanning electron microscope (FEG-SEM FEI Inspect F50). Thermal etching was also carried out at 1500 °C/20 min.

The electrical properties of the sintered pellets were evaluated by impedance spectroscopy (IS) in a Hewlett Packard 4192A impedance analyzer in the 400–700 °C range. The IS data were collected in the 5 Hz to 1.3×10^7 Hz frequency range, 200 mV input signal. Silver electrodes were applied onto the parallel surfaces of the pellets. The IS diagrams were normalized by the geometrical factors (S/l , S =electrode area, l =pellet thickness) of the pellets.

3. Results and discussion

3.1. Powder synthesis and characterization

The synthesis of ceramic powders by the OP route is known to occur due to oxi-reduction reactions of cations in presence of an inorganic peroxo-complex. For yttrium-doped barium zirconate, the formation of the precipitate occurs due to cation hydrolysis in an alkaline peroxide hydrogen mixture, since no oxidation state changed either during the synthesis or during heat treatment. To ensure the control of Ba(II) stoichiometry another modification has been done regarding the way that the cation solution is added into the oxidant mixture. The addition was fast enough to minimize the reaction between the barium nitrate solution and carbonic acid (H₂CO₃), formed during CO₂ dissolution in water (1) [31]. This reaction (2) allows the formation of BaCO₃ and may cause further stoichiometry deviation, empirically verified.

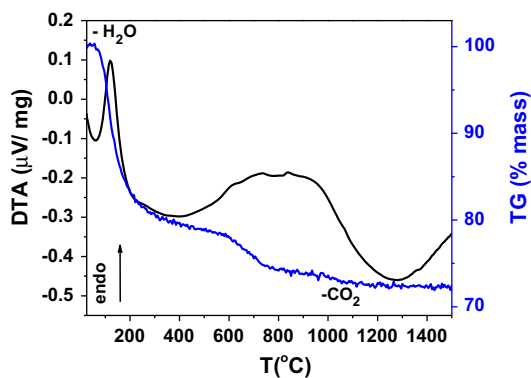


Fig. 1. Thermogravimetric and differential thermal analysis curves of the precursor powder synthesized by the oxidant-peroxo (OP) method.

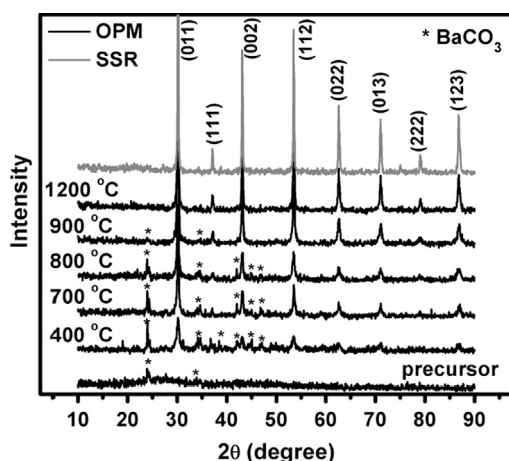


Fig. 2. X-ray diffraction patterns of BZY powders synthesized by the oxidant-peroxo (OP) method and by the solid state reaction (SSR) route.

Table 1

Compositions determined by X-ray fluorescence analysis and lattice parameters of BZY powders synthesized by the oxidant-peroxo (OP) method and solid state reaction (SSR) route and heat treated at different temperatures. (Composition data normalized in moles of cation per formula unit).

Synthesis route	Calcination (°C/h)	Stoichiometric ratio			Lattice parameter $a=b=c$ (Å) ± 0.0001
		Ba ± 0.02	Zr ± 0.03	Y ± 0.01	
OP	700/4	1.03	0.89	0.11	4.1898
	800/4	1.07	0.89	0.11	4.1964
	900/4	1.08	0.89	0.11	4.1918
SSR	1200/2	1.05	0.89	0.11	4.1989
	2x 1250/24	0.93	0.89	0.11	4.2326

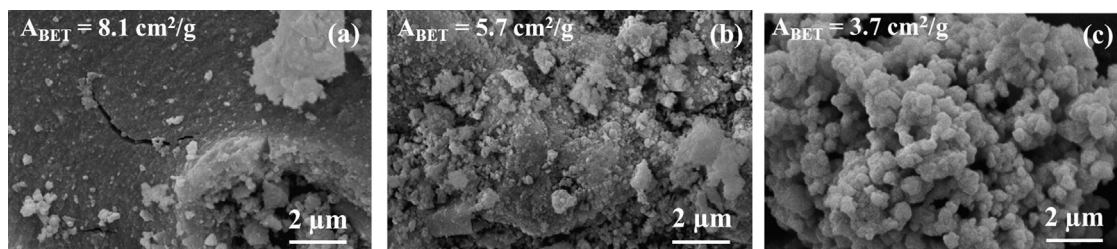
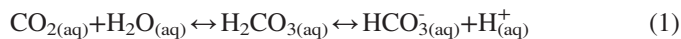


Fig. 3. SEM images of powders synthesized by the oxidant-peroxo (OP) method calcined at (a) 900 °C/4 h and (b) 1200 °C/2 h, and (c) powder prepared by the solid state reaction (SSR) route. The specific surface areas are indicated.



The established experimental procedure promoted the formation of a white $\text{Ba}(\text{Zr}_{0.89}\text{Y}_{0.11})\text{O}_{3-\delta}$ precipitate, the molar content being evaluated by X-ray fluorescence analysis.

The thermal behavior of the precursor powder was monitored by thermogravimetric and differential thermal analyses, shown in Fig. 1.

The first endothermic process takes place in the 60–200 °C range, due to the release of the physically adsorbed and chemically bonded water, accompanied by a 20% mass loss. The second step in the 600–750 °C range is probably due to the decomposition of peroxide groups (O_2^{2-}) by endothermic release of oxygen and consists on the major mass loss [32]. There is also a small endothermic peak at approximately 830 °C, which has been ascribed to phase transitions that occur on the low content of physically adsorbed BaCO_3 [33,34]. A small mass loss happens in the 800–1200 °C range, probably related to BaCO_3 complex carbonate [17]. Based on the BaZrO_3 synthesis by the peroxide route [32] and the thermal behavior of the precursor obtained by the OP method (Cf. Fig. 1), the chemical formula of the precursor powder has been estimated as $8\text{BaZr}_{0.89}\text{Y}_{0.11}\text{O}_{3-\delta} \cdot 3(\text{O}_2) \cdot 32\text{H}_2\text{O}$.

Fig. 2 shows the results of the X-ray diffraction analysis of the powders obtained by both OP and SSR routes. The precursor powder is amorphous. The figure shows the crystalline barium carbonate phase formed during the synthesis, due to the reaction of $\text{Ba}(\text{II})$ solution with carbon dioxide. The cubic perovskite phase could be indexed (PDF 6–399, $a=4.193$ Å) after heat

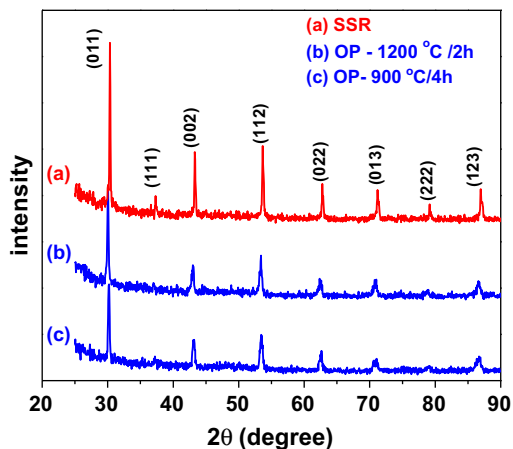


Fig. 4. X-ray diffraction patterns of pellets produced with powders obtained by the solid state reaction (SSR) route (a) and the oxidant-peroxo (OP) method calcined at 1200 °C (b) and 900 °C (c). Pellets sintered at 1600 °C/4 h.

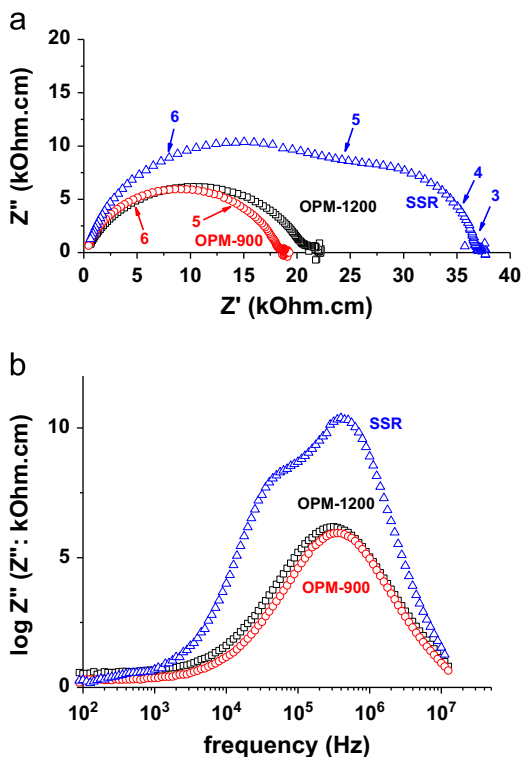


Fig. 5. Impedance plots (a) and Bode diagrams (b) of BZY10 pellets measured at 600 °C.

treating the precursor powder at temperatures higher than 400 °C. However, single phase was achieved only after heating at 1200 °C. Similar results were reported on powders produced by spray pyrolysis [17]. The powders produced by the solid state reaction also produced single phase powders.

Table 1 shows the composition of each sample evaluated by X-ray fluorescence analysis. The Zr/Y ratio is equal for all samples, 89/11. The oxidant-peroxo method promoted the formation of stoichiometric BZY10 powders without barium loss. The powders obtained by solid state reaction present less than 0.1% barium loss. In spite of this fact, the perovskite

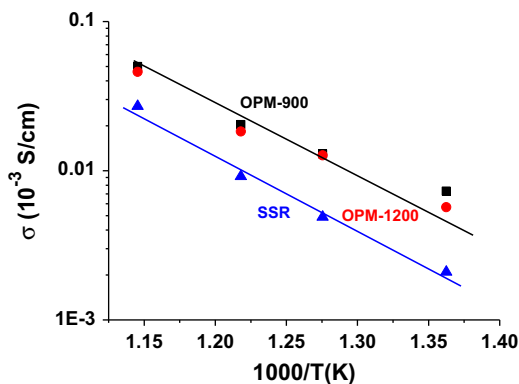


Fig. 6. Arrhenius plots of total conductivity of yttrium-doped barium zirconate pellets prepared by the oxidant-peroxo (OP) method and by the solid state reaction (SSR) route.

structure is able to accommodate up to 0.08% of barium deficiency, which explains the absence of secondary phases in the X-ray diffraction patterns of the sample produced by solid state reaction [18]. The lattice parameter was evaluated and the results are presented in Table 1. The lattice parameter of the OP powders increases for increasing the heat treating temperature, probably due to the release of BaCO₃ [15]. The highest value (4.1989 Å), similar to the reported value in the PDF 6–399, was obtained for the powders heated at 1200 °C. The lattice parameter of the powder obtained by solid state reaction is higher than the corresponding value in the PDF 6–399. This is expected, according to the Vegard law, for an ideal composition since the Zr⁴⁺ cation is substituted for the larger Y³⁺ cation ($R_{Zr}^{4+} = 0.72 \text{ \AA}$; $R_Y^{3+} = 0.90 \text{ \AA}$ [35]). The defect chemistry may also be affected by barium deficiency. Some authors consider the partitioning of the dopant over the two A and B sites, which can lead to a decrease of the cell volume relative to a stoichiometric composition, but this effect holds to a much lesser extent than Y³⁺ replacing Zr⁴⁺ on the B-site [36].

Fig. 3 shows scanning electron microscopy images of BZY10 powders produced by the OP route after heating to 900 °C, 1200 °C, and synthesized by solid state reaction. Heating the powders produced by the oxidant-peroxo method leads to spherical nanoparticles in the agglomerate state. The SSR powders are also agglomerates, but of submicron particles. The specific surface areas are depicted in each image but they actually represent agglomerate values. The specific surface area of OPM powders is lower than the ones of powders produced by other chemical synthesis such as sol–gel [1] and spray pyrolysis [20].

3.2. Pellet characterization

Fig. 4 shows the results of the X-ray diffraction analysis of sintered pellets prepared with powders synthesized by the OP and SSR routes. Only the single cubic perovskite phase is detected, irrespective of the initial barium carbonate content.

The sintered pellets reached the following relative densities: 91% and 94% (from OPM powders calcined at 1200 °C and 900 °C, respectively); 88% (SSR powders). Despite the high

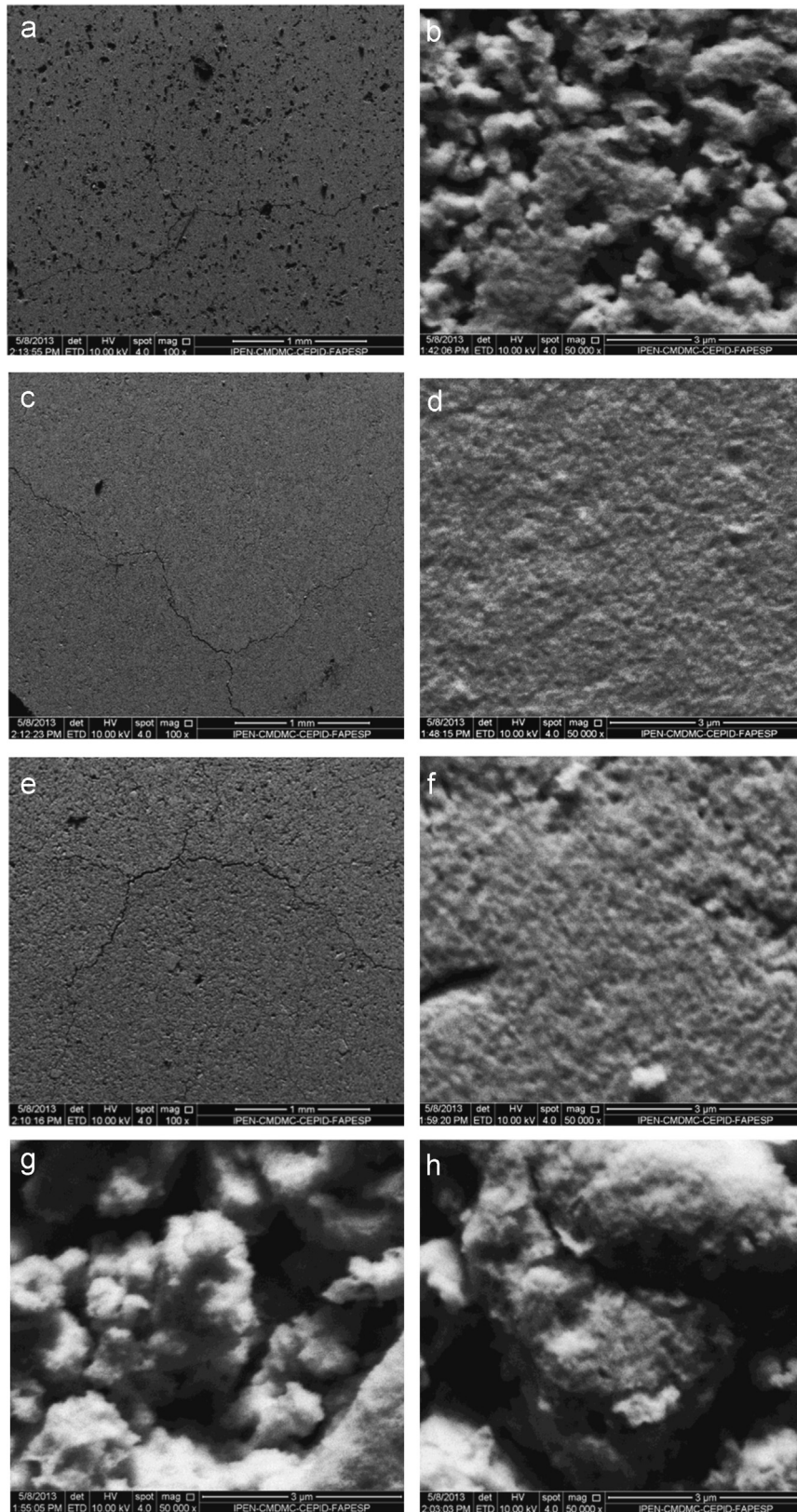


Fig. 7. Scanning electron microscopy micrographs of thermally etched surfaces of sintered BZY10 prepared with: (a and b)—solid state reaction (SSR) powders; (c, d and g) - oxidant-peroxo (OP) method (calcined at 900 °C); (e, f and h) - oxidant-peroxo (OP) method (calcined at 1200 °C). Dense region: (d and f); non dense region: (g and h). See text for details.

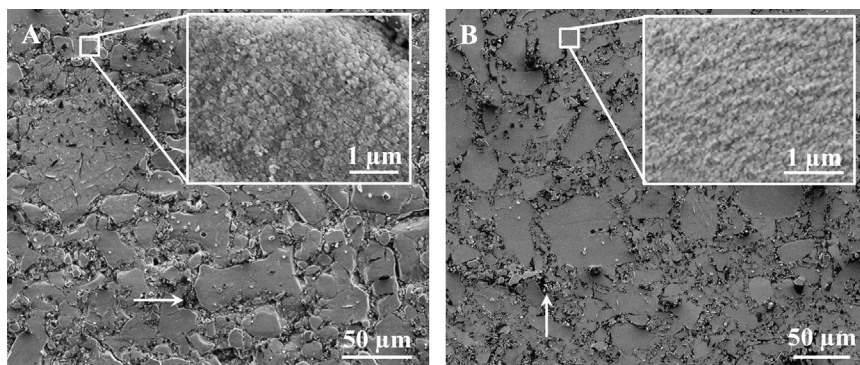


Fig. 8. FEG-SEM images of polished and chemically etched surfaces of BZY10 pellets. The powders were synthesized by the oxidant-peroxo (OP) method and heat treated at (A) 900 °C for 4 h and (B) 1200 °C for 2 h; inset: nanosized cubic grains.

agglomeration of the powders obtained by the oxidant-peroxo method, the pellets achieved higher relative density in sintering time shorter than the ones reported using powders also synthesized by chemical routes [20,37–39].

The composition of the pellets was evaluated by X-ray fluorescence analysis. All samples have the same composition ($\text{Ba}_{1.08}\text{Zr}_{0.89}\text{Y}_{0.11}\text{O}_{3-\delta}$), probably an equilibrium composition due to mass transport provided by the powder in which the pellets had been embedded.

Fig. 5 shows the results of the electrical measurements of the three pellets in two representations: the imaginary component as a function of the real component of the impedance and the dependence of the imaginary component on the frequency (Bode diagram).

A single semicircle has been resolved [37,40,41]. A typical grain boundary capacitance value (10^{-11} F/cm) was determined from the analysis of the impedance plots [20]. The blocking of charge carriers at interfaces (mainly grain boundaries) remains the main contribution to the electrical resistivity. The Arrhenius plots of the total conductivity are presented in Fig. 6. The total conductivity of the pellets sintered with powders synthesized by the oxidant-peroxo method is 2.4 times larger comparing with pellets sintered with powders obtained by solid state reaction.

Fig. 7 shows FEG-SEM micrographs of thermally etched surfaces of sintered pellets of three kinds: using powders synthesized by the OP method calcined at 900 °C and at 1200 °C, and using powders synthesized by the solid state route. Sintered pellets using powders synthesized by the OP method present typically two main regions: one dense with large grains consisting of submicron subgrains, and another with pores. The cracks, visible in the low magnitude images, are due to the thermal shock during the thermal etching, not seen in the chemically etched specimens (see Fig. 8).

Fig. 8 shows FEG-SEM micrographs of BZY10 polished and chemically etched surfaces of pellets sintered at 1600 °C using powders synthesized by the OP method followed by calcination at (A) 900 °C for 4 h and (B) 1200 °C for 2 h. There are two regions in the images: (i) porous, indicated by arrows; (ii) flat and dense. The former it is composed by densely packed cubic grains (inset), mainly when the powders were calcined at 1200 °C. The average dimension of the cubic

grains is estimated in the 50–100 nm range. This relatively small grain size is consistent with the highly refractory nature of BYZ, which shows low rates of grain growth under typical sintering conditions [13]. Images of specimens thermally etched are similar, besides the presence of thermal shock produced cracks.

4. Conclusions

A simple, cost-effective and clean method of ceramic powder synthesis, based on the oxidant-peroxo method, was successfully established for the synthesis of yttrium-doped barium zirconate. Among the advantages over other methods, it provides good control of the barium stoichiometry, the particles are sinteractive and the particle sizes are in the nanosize range. Even though porous intergranular regions remain responsible for blocking proton conduction, the sintered pellets produced with these powders achieved total electrical conductivity 2.4 times the conductivity measured in pellets of powders obtained by solid state synthesis and relative density higher than 91% of the theoretical density.

Acknowledgments

To Dr. J. R. Martinelli for the XRF analyses. One of the authors (MDG) acknowledges FAPESP for the Doctorate scholarship (Proc. 2011/50197-0).

References

- [1] Y. Yamazaki, R. Hernandez-Sanchez, S.M. Haile, *Chemistry of Materials* 21 (2009) 2755–2762.
- [2] Y. Guo, R. Ran, Z. Shao, *International Journal of Hydrogen Energy* 36 (2011) 1683–1691.
- [3] S.M. Haile, *Acta Materialia* 51 (2003) 5981–6000.
- [4] A. Orera, P.R. Slater, *Chemistry of Materials* 22 (2010) 675–690.
- [5] H. Ding, J. Ge, X. Xue, *Electrochemical Solid State Letters* 15 (2012) B86–B89.
- [6] B.C.H. Steele, A. Heinzel, *Nature* 414 (2001) 345.
- [7] L. Bi, E. Fabbri, E. Traversa, *Electrochemistry Communications* 16 (2012) 37–40.
- [8] A. Slodczyk, P. Colomban, D. Lamago, G. André, O. Zafarani, O. Lacroix, A. Sirat, F. Grasset, B. Sala, *Journal of Materials Research* 27 (2012) 1939–1949.

- [9] H. Iwahara, Y. Asakura, K. Katakiram, M. Tanaka, *Solid State Ionics* 168 (2004) 299–310.
- [10] K. Xie, R. Yan, X. Xu, X. Liu, G. Meng, *Materials Research Bulletin* 44 (2009) 1474–1480.
- [11] K.D. Kreuer, *Annual Review of Materials Research* 33 (2003) 333–359.
- [12] E.C.C. Souza, R. Muccillo, *Materials Research* 13 (2010) 385–394.
- [13] P. Babilo, S.M. Haile, *Journal of the American Ceramic Society* 88 (2005) 2362–2368.
- [14] S.B.C. Duval, P. Holtappels, U.F. Vogt, E. Pomjakushina, K. Conder, U. Stimming, T. Graule, *Solid State Ionics* 178 (2007) 1437–1441.
- [15] A. Magrez, T. Schober, *Solid State Ionics* 175 (2004) 585–588.
- [16] Y. Yamazaki, P. Babilo, S.M. Haile, *Chemistry of Materials* 20 (2008) 6352–6357.
- [17] S.B.C. Duval, P. Holtappels, U.F. Vogt, U. Stimming, T. Graule, *Fuel Cells* 9 (2009) 613–621.
- [18] Y. Yamazaki, R. Hernandez-Sanchez, S.M. Haile, *Journal of Materials Chemistry* 20 (2010) 8158–8166.
- [19] B. Bendjeriou-Sedjerari, J. Loricourt, D. Goeuriot, P. Goeuriot, *Journal of Alloys and Compounds* 509 (2011) 6175–6183.
- [20] P.I. Dahl, H.L. Lein, Y. Yu, J. Tolchard, T. Grande, M.-A. Einarsrud, C. Kjølseth, T. Norby, R. Haugsrud, *Solid State Ionics* 182 (2011) 32–40.
- [21] E.R. Camargo, J. Frantti, M. Kakihana, *Journal of Materials Chemistry* 11 (2001) 1875–1879.
- [22] E.R. Camargo, M. Popa, J. Frantti, M. Kakihana, *Chemistry of Materials* 13 (2001) 3943–3948.
- [23] E.R. Camargo, F.L. Souza, E.R. Leite, M. Kakihana, *Journal of Applied Physics* 96 (2004) 2169–2172.
- [24] A.H. Pinto, F.L. Souza, A.J. Chiquito, E. Longo, E.R. Leite, E.R. Camargo, *Materials Chemistry and Physics* 124 (2010) 1051–1056.
- [25] A.H. Pinto, F.L. Souza, E. Longo, E.R. Leite, E.R. Camargo, *Materials Chemistry and Physics* 130 (2011) 256–263.
- [26] K.D. Kreuer, S. Adams, W. Munch, A. Fuchs, U. Klock, J. Maier, *Solid State Ionics* 145 (2001) 295–306.
- [27] A. Radojković, M. Žunic, S.M. Savić, G. Branković, Z. Branković, *Ceramics International* 39 (2013) 307–313.
- [28] A. Radojković, M. Žunic, S.M. Savić, G. Branković, Z. Branković, *Ceramics International* 39 (2013) 2631–2637.
- [29] Y. Liu, Y. Guo, R. Ran, Z. Shao, *Journal of Membrane Science* 415 (2012) 391–398.
- [30] (<http://www.ccp14.ac.uk/ccp/web-mirrors/crush/astaff/holland/UnitCell.html>).
- [31] A.I. Vogel, *Textbook of macro and semimicro qualitative inorganic analysis*, 5th ed., Longman, New York, 1979.
- [32] G. Pfaff, *Materials Letters* 32 (1995) 393–397.
- [33] E. Antonelli, M.I. Bernardi, A.C. Hernandez, *Cerâmica* 51 (2005) 428–433.
- [34] H.-L. Lin, R.-K. Chiang, C.-L. Kuo, C.-W. Chang, *Journal of Non-Crystalline Solids* 353 (2007) 1188–1194.
- [35] R.D. Shannon, *Acta Crystallographica, Section A: Foundations of Crystallography* 32 (1976) 751–767.
- [36] Y. Yamazaki, C.-K. Yang, S.M. Haile, *Scripta Materialia* 65 (2011) 102–107.
- [37] P. Babilo, T. Uda, S.M. Haile, *Journal of Materials Research* 22 (2007) 1322–1330.
- [38] E. Fabbri, D. Pergolesi, S. Licocchia, E. Traversa, *Solid State Ionics* 181 (2010) 1043–1051.
- [39] Z. Sun, E. Fabbri, L. Bi, E. Traversa, *Journal of the American Ceramic Society* 95 (2011) 627–635.
- [40] H.G. Bohn, T. Schober, *Journal of the American Ceramic Society* 83 (2000) 768–772.
- [41] S. Tao, J.T.S. Irvine, *Journal of Solid State Chemistry* 180 (2007) 3493–3503.